Journal of Alloys and Compounds 375 (2004) 24–30

Journal of ALLOYS AND COMPOUNDS

www.elsevier.com/locate/jallcom

Synthesis, crystal structure and Mössbauer effect studies of $Dy(Mn_{0.4}Fe_{0.6-x}Al_x)_2$ intermetallics

P. Stoch [a], J. Pszczoła [a,*], P. Jagodziński [a], A. Jabłońska [b], J. Suwalski [b], L. Dąbrowski [b], A. Pańta [c]

[a] *Solid State Physics Department, AGH, Al. Mickiewicza 30, 30-059 Kraków, Poland*
[b] *Institute of Atomic Energy, 05-400 Świerk-Otwock, Poland*
[c] *Department of Metallurgy and Materials Engineering, AGH, Al. Mickiewicza 30, 30-059 Kraków, Poland*

Received 10 October 2003; received in revised form 15 November 2003; accepted 15 November 2003

Abstract

It was previously found, that the magnetic hyperfine fields observed at ^{57}Fe nuclei (4.2 K) in the $Dy(Mn_{1-x}Fe_x)_2$ and $Dy(Fe_{1-x}Co_x)_2$ intermetallics form a Slater–Pauling curve. Both 3d sub-bands in the $Dy(Mn_{0.4}Fe_{0.6})_2$ compound are filled up only partially with 3d electrons. The consequence of Fe/Al substitution, in the $Dy(Mn_{0.4}Fe_{0.6})_2$ compound, was studied in the present paper. For this purpose the synthesis and X-ray analysis (300 K) of the series $Dy(Mn_{0.4}Fe_{0.6-x}Al_x)_2$ were performed. The cubic, $MgCu_2$-type, Fd3m crystal structure was observed across the series. ^{57}Fe Mössbauer effect measurements for the series were realized at 4.2 K. The obtained crystallographic data and the hyperfine interaction parameters are presented. The magnetic hyperfine fields form a separate branch of the Slater–Pauling curve. The data are qualitatively related to the Stoner model.

Keywords: Intermetallics; Crystal structure; ^{57}Fe Mössbauer effect; Hyperfine interactions; Slater–Pauling curve; Band structure

1. Introduction

The heavy rare earth (R) transition metal (M) ferrimagnets (RM_2) are widely studied for their fundamental interest and their practical applications [1–3]. Ferrimagnetism of the RM_2 compounds results from the coexistence between the 4f (5d) and 3d-electron magnetism [4–6]. The electronic band structure of these intermetallics, and in particular of their transition metal sublattice, is rather complex and poorly understood up to date.

Systematic Mössbauer effect measurements of the substituted RM_2 intermetallic series can be treated as a suitable method to study both the rare earth and the transition metal sublattice and thus to clarify the 3d-5d-4f magnetism. It was previously found, that the magnetic hyperfine fields $\mu_0 H_{hf}$ (μ_0 is the magnetic permeability), studied at ^{57}Fe nuclei in the $Dy(Mn_{1-x}Fe_x)_2$ and $Dy(Fe_{1-x}Co_x)_2$ intermetallic series, treated as a function of the average number n of 3d electrons calculated per transition metal site (analogously to the 3d metal–3d metal alloys [7–9]) behave according to the Slater–Pauling curve with a maximum hyperfine field occuring for the $Dy(Fe_{0.7}Co_{0.3})_2$ compound [5,6].

Across the $Dy(Mn_{1-x}Fe_x)_2$ series the magnetic hyperfine field $\mu_0 H_{hf}$ increases with x (or n). In this case, both the 3d sub-bands are filled-up step by step against x and for this series a completeness of both the sub-bands is not reached.

Al substitution is usually treated as a useful method to modify the magnetic properties and hyperfine interactions and thus to probe indirectly the band structure of the R–M compounds. As a result of the Al substitution the $3d^6 4s^2$ electrons of iron atoms are gradually replaced by the $3s^2 p^1$ electrons of aluminium atoms. This change strongly influences the 3d band and thus the magnetism and hyperfine interactions of the compounds [10–14].

It would be interesting to study the significance of the iron component alone in the compounds, with the 3d sub-bands only partially occupied by 3d electrons. In other words, to study a series of compounds with a constant Mn-contribution and with a gradually reduced Fe-contribution. Therefore, in order to test the influence of the iron atoms on the 4f-5d-3d

* Corresponding author.
E-mail address: pszczola@uci.agh.edu.pl (J. Pszczoła).

0925-8388/$ – see front matter © 2003 Elsevier B.V. All rights reserved.
doi:10.1016/j.jallcom.2003.11.024

magnetism and especially on the magnetism of the 3d sublattice, Fe/Al substitution in the $Dy(Mn_{0.4}Fe_{0.6-x}Al_x)_2$ series was used in the present paper. The intermetallics $Dy(Mn_{0.4}Fe_{0.6-x}Al_x)_2$ were synthesized and then detailed X-ray crystallographic studies and ^{57}Fe Mössbauer effect measurements were performed. The obtained data are qualitatively discussed within the frame of the rigid band model [9,15,16].

2. Synthesis of materials

The new series of intermetallic compounds $Dy(Mn_{0.4}Fe_{0.6-x}Al_x)_2$ ($x = 0$, 0.1, 0.2, 0.3, 0.4, 0.5 and 0.6) was prepared by arc melting [17], in a high purity argon atmosphere from the appropriate amounts of Dy (99.9% purity), Mn, Fe and Al (all 99.999% purity) as starting materials.

As an example, the influence of the duration time t of the annealing (at 1200 K in argon atmosphere) on the crystal structure was tested for the $Dy(Mn_{0.4}Fe_{0.6})_2$ starting compound of the series. For this purpose the $Dy(Mn_{0.4}Fe_{0.6})_2$ separate samples being parts of the same melt were heated at different times: $t = 0$–19 h. The X-ray patterns obtained for these samples were analysed using the Rietveld-type procedure [18–20]. For all the heated samples the cubic, Fd3m, $MgCu_2$-type (C15) Laves phases [21–23] were observed.

As a result of the heat treatment (duration time $t > 0$), the lattice parameter a initially increases slightly as compared to the parameter of the unheated sample. Moreover, it seems that there is no further change of the a parameter versus t. Even short heating reduces considerably the half-widths Γ of the X-ray reflections as compared to the half-widths of the unheated sample.

Considering the above mentioned data, all the synthesized compounds $Dy(Mn_{0.4}Fe_{0.6-x}Al_x)_2$ were commonly heated at 1200 K during 19 h in a high purity argon atmosphere. For all the compounds, a single crystallographic phase corresponding to the cubic, Fd3m, $MgCu_2$-type (C15) Laves phase (described in detail in refs. [21,22]) was obtained.

Here, it is worth noticing that the $MgCu_2$-type unit cell contains eight stoichiometric formula units, i.e. 24 atoms: 8 Mg and 16 Cu atoms. It will be useful below to mention that each Cu (or transition metal atom M) has six Cu (or M) atoms in the nearest neighbour shell (radius $a(2)^{1/2}/4$) [22].

The lattice parameters $a(x)$ with errors resulting from the fitting procedure and the calculated distance $d_{M–M}$ between nearest neighbours in the transition metal sublattice, the unit cell volume V and the volume w per atom are presented in Table 1 (the value at $x = 0$ estimated from data of the $Dy(Mn_{1-y}Fe_y)_2$ series is added [24]). Actually, it is expected that physical errors should be somewhat higher, mainly due to possible but low deviations Δx of the composition parameters of the compounds.

Table 1
Crystallographic data for the $Dy(Mn_{0.4}Fe_{0.6-x}Al_x)_2$ series (300 K)

x	a (Å)	$d_{M–M}$ (Å)	V (Å^3)	w (Å^3)
0	7.3913 (14), 7.372 (2) [24]	2.6132	403.7 (5)	16.89 (2)
0.1	7.4597 (6)	2.6374	415.2 (3)	17.30 (1)
0.2	7.5187 (9)	2.6582	425.1 (4)	17.78 (2)
0.3	7.5842 (8)	2.6814	436.2 (4)	18.18 (2)
0.4	7.6516 (10)	2.7052	448.0 (4)	18.67 (2)
0.5	7.7275 (9)	2.7320	461.4 (4)	19.23 (2)
0.6	7.7954 (6)	2.7560	473.6 (3)	19.73 (1)

Note: a, unit cell parameter; $d_{M–M}$, distance between nearest neighbours in the transition metal sublattice; V, unit cell volume and w, volume per atom.

3. Mössbauer effect studies

3.1. Spectra and analysis

The Mössbauer effect measurements were performed at 4.2 K by using a standard transmission technique with a source of ^{57}Co in Rh.

The ^{57}Fe Mössbauer effect spectra successfully observed experimentally for the $Dy(Mn_{0.4}Fe_{0.6-x}Al_x)_2$ intermetallics are presented in Fig. 1. As these spectra are composed of a number of subspectra they are weakly resolved. This complexity should be mainly related to the different, presumably random (Mn, Fe, Al) nearest neighbour (n.n.) surroundings of the observed Fe atom resulting from the Fe/Al substitution. Each (Mn, Fe, Al) n.n. surrounding introduces its own subspectrum and thus its own set of hyperfine interaction parameters. The n.n. surrounding is composed of n_1 Mn atoms, n_2 Fe atoms and n_3 Al atoms, with a crystal lattice

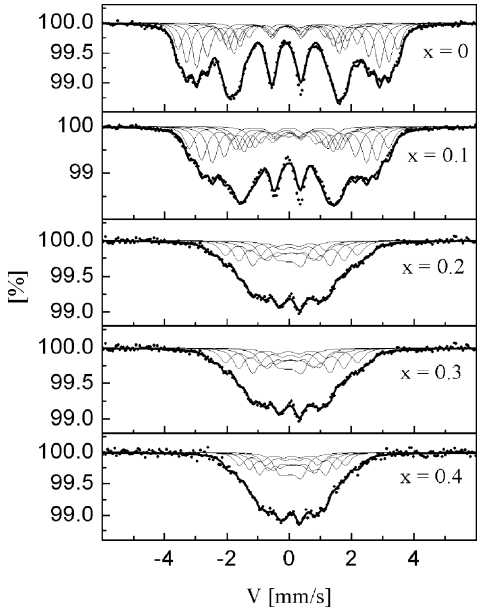

Fig. 1. ^{57}Fe Mössbauer effect transmission spectra of the $Dy(Mn_{0.4}Fe_{0.6-x}Al_x)_2$ intermetallics (4.2 K). Experimental points, fitted lines and fitted subspectra are presented.

Table 2
Fitted data for the exemplary $Dy(Mn_{0.4}Fe_{0.4}Al_{0.2})_2$ compound

n_1, n_2, n_3	$P(n_2)$	$W(n_2)$	G (mm/s)	IS (mm/s)	$\mu_0 H_{hf}$ (T)	QS (mm/s)
5, 1, 0	0.20139	0.15537	0.261	0.084 (25)	3.81 (11)	−0.048 (23)
4, 1, 1						
3, 1, 2						
2, 1, 3						
4, 2, 0	0.31250	0.11698	0.261	0.235 (27)	7.20 (8)	−0.087 (29)
3, 2, 1						
2, 2, 2						
3, 3, 0	0.30092	0.23274	0.261	0.128 (12)	9.79 (7)	0.021 (11)
2, 3, 1						
1, 3, 2						
2, 4, 0	0.13889	0.19342	0.261	0.129 (22)	12.21 (8)	0.031 (23)
1, 4, 1						
1, 5, 0	0.04167	0.15537	0.261	0.101 (12)	14.71 (7)	0.012 (12)
0, 5, 1						
0, 6, 0	0.00463	0.12109	0.261	0.044 (31)	17.01 (1)	0.055 (29)
Average values				0.116 (20)	10.42 (7)	0.002 (19)
$\chi^2 = 0.913$ MISFIT $= (0.066 \pm 0.031)\%$						

Note: n_1, n_2 and n_3 are the numbers of Mn, Fe, and Al atoms, respectively; $P(n_2)$ and $W(n_2)$ are probabilities and weights of subspectra; G is 0.5 of the half-width of the Mössbauer line; IS, $\mu_0 H_{hf}$, QS are the hyperfine interaction parameters (at 4.2 K); χ^2 and MISFIT are defined for instance in [30].

condition for these numbers $n_1+n_2+n_3 = 6$. Assuming that the transition metal sublattice in the $Dy(Mn_{0.4}Fe_{0.6-x}Al_x)_2$ intermetallics is randomly populated by Mn, Fe and Al atoms with probabilities of $p_1 = 0.4$, $p_2 = (0.6 - x)$ and $p_3 = x$ ascribed to the Mn, Fe and Al atoms, respectively ($p_1 + p_2 + p_3 = 1$), the probabilities $P(\{6; n_1, n_2, n_3\})$ of the particular n.n. surroundings $\{6; n_1, n_2, n_3\}$ can be calculated using the general Bernoulli formula for intermediate compounds of the series, or using the ordinary Bernoulli formula for the borderline compounds of the series [25]. There is too big a number of different n.n. surroundings $\{6; n_1, n_2, n_3\}$ and the corresponding probabilities $P(\{6; n_1, n_2, n_3\})$ to consider all of them during a fitting procedure. Therefore a simplification should be made. Fortunately there is a big group of vanishingly small probabilities which are calculated following the Bernoulli formulae. These can be omitted. It was assumed that the magnetically most important constituents are the Fe atoms. The remaining probabilities, considering the last assumption, were grouped and after that used to define the probabilities $P(n_2 = i)$, i.e. the probabilities to find a number i of Fe atoms in the n.n. surroundings, namely $P(n_2 = i) = \Sigma P(\{n_1, i, n_3\})$ where summarization is taken over the set of numbers $\{n_1, n_2 = i, n_3\}$ (as shown in Table 2 for exemplary compound). During the fitting procedure, it was assumed that the starting amplitudes $A(n_2)$ and thus the weights of subspectra: $W(n_2) = A(n_2)/\Sigma A(n_k)$ follow the probabilities $P(n_2)$. Sometimes it is important to consider also the direction of the [1 1 1] easy axis of magnetization during the fitting procedure, which introduces additional complexity of spectra [26–29]. After a number of different fitting trials, the simpler case, the [1 0 0] easy axis of magnetization was assumed to exist for all the subspectra [26]. Following this way it was possible to obtain reasonable fits. Exemplary fitted results for $Dy(Mn_{0.4}Fe_{0.4}Al_{0.2})_2$ are presented in Table 2 (including χ^2 parameter and MISFIT [30]). Actually, it is impossible during the numerical analysis to consider all the factors reflecting the physical complexity of the problem. For instance, the influence of the next nearest neighbour configurations, and a possible deviation from randomness were not taken into account and thus some arbitrariness of the fitting procedure cannot be avoided. As a result, some differences between $P(n_2)$ (shaded rectangles) and $W(n_2)$ (open rectangles) are observed (Fig. 2). It can be seen that the difference between the $P(n_2)$ distribution and

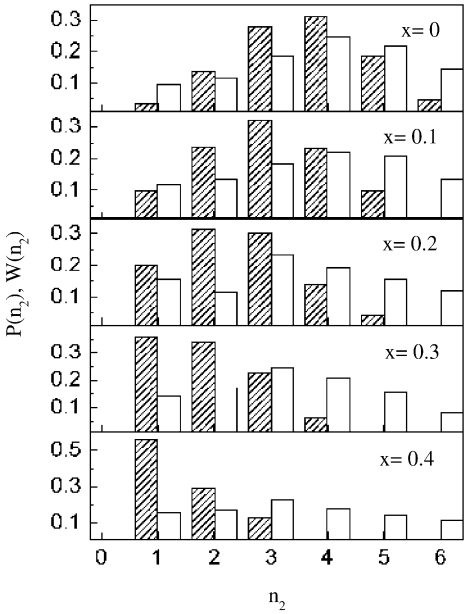

Fig. 2. Probabilities $P(n_2)$ (shaded rectangles) and weights $W(n_2)$ (open rectangles) of the particular subspectra against the number n_2 of the Fe atoms as nearest neighbours for the series $Dy(Mn_{0.4}Fe_{0.6-x}Al_x)_2$.

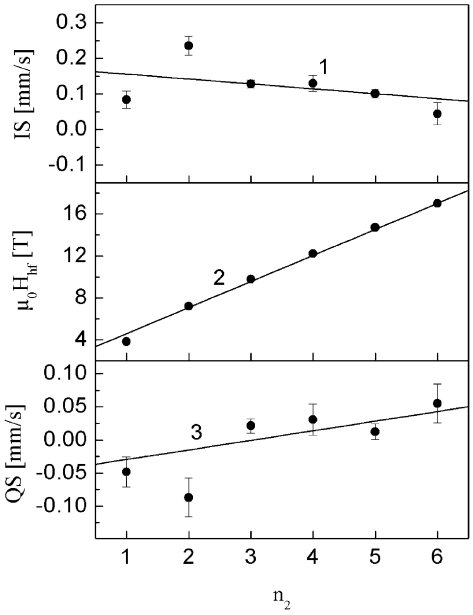

Fig. 3. Hyperfine interaction parameters for different subspectra (against n_2) of the exemplary $Dy(Mn_{0.4}Fe_{0.4}Al_{0.2})_2$ compound (4.2 K): (1) the isomer shift IS in relation to Fe-metal, 300 K; (2) the magnetic hyperfine field μ_0H_{hf} and (3) the quadrupole interaction parameter QS.

the $W(n_2)$ distribution increases with x. Nevertheless, taking into account the complexity of the spectra and thus of the fitting procedure, the probabilities $P(n_2)$ and the weights $W(n_2)$ seem to be relatively similar.

3.2. Local hyperfine interaction parameters versus n_2

From the numerical analysis, the hyperfine interaction parameters corresponding to particular weights (or n_2), i.e. the isomer shift IS(n_2) (with respect to pure iron metal, at 300 K), the magnetic hyperfine field $\mu_0H_{hf}(n_2)$ and the quadrupole interaction parameter QS(n_2) (QS = eqQ/4 [31]) were determined for all the studied compounds of the series.

The data for the exemplary $Dy(Mn_{0.4}Fe_{0.4}Al_2)_2$ compound are presented in Fig. 3. The fitted isomer shift slightly decreases with n_2, namely $IS(n_2) = (-0.014n_2 + 0.170)$ mm/s. The magnetic hyperfine field increases: μ_0H_{hf} $(n_2) = (2.49n_2 + 2.10)$ T, and the quadrupole parameter slightly increases: $QS = (0.014n_2 - 0.044)$ mm/s.

The magnetic hyperfine field arithmetically averaged across the $Dy(Mn_{0.4}Fe_{0.6-x}Al_x)_2$ series increases linearly with n_2, μ_0H_{hf} $(n_2) = (2.42n_2 + 3.12)$ T, and it can be seen in Fig. 4. Following the fitted line it can be found that for a lack of iron atoms as n.n. the magnetic field originated by the rest of crystal lattice equals μ_0H_{hf} $(n_2 = 0) = 3.12$ T. Analogously for six iron atoms as n.n. the field equals μ_0H_{hf} $(n_2 = 6) = 17.65$ T. It can be added that the average increasing rate equals 2.42 T per one Fe atom as nearest neighbour. This value is relatively close to the rate previously observed for the $Dy(Fe_{1-x}Al_x)_2$ series which equals

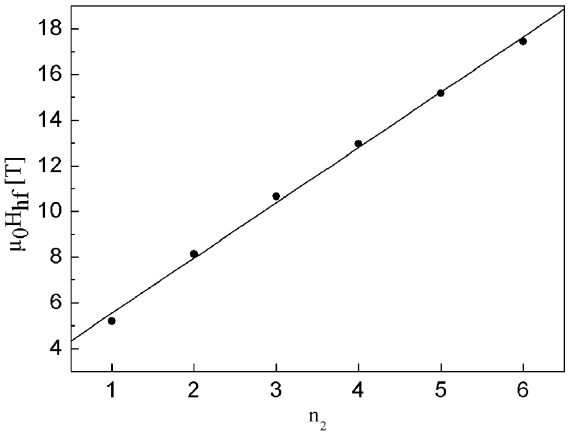

Fig. 4. The magnetic hyperfine field $\mu_0H_{hf}(n_2)$ arithmetically averaged across the $Dy(Mn_{0.4}Fe_{0.6-x}Al_x)_2$ series (4.2 K).

2.57 T per Fe atom as n.n. [11]. For the last series, the counterpart to μ_0H_{hf} ($n_2 = 0$) equals 5.7 T and the counterpart to μ_0H_{hf} ($n_2 = 6$) equals 21.12 T [11]. Following these compared data, it can be seen that the field dependence $\mu_0H_{hf}(n_2)$ observed for the $Dy(Mn_{0.4}Fe_{0.6-x}Al_x)_2$ series is situated considerably below the field dependence previously observed for the $Dy(Fe_{1-x}Al_x)_2$ series (not shown in Fig. 4) [11]. This downward shift can be mainly related to the presence of manganese atoms in the transition metal sublattice of the $Dy(Mn_{0.4}Fe_{0.6-x}Al_x)_2$ series.

3.3. Average hyperfine interaction parameters versus x

The average values of the hyperfine interaction parameters (calculated following formula: $X = (\Sigma W_i X_i)/\Sigma W_k$), i.e., the isomer shift IS (with respect to pure iron metal, at 300 K), the magnetic hyperfine field μ_0H_{hf} and the quadrupole interaction parameter QS obtained for the $Dy(Mn_{0.4}Fe_{0.6-x}Al_x)_2$ series, are presented in Fig. 5. Moreover, the values of parameters are listed in Table 3. Additionally, the previous literature data for $x = 0$ are included in the figure [24].

The average isomer shift $IS(x) = 0.070(9)$ mm/s at $x = 0$, increases linearly across the series $Dy(Mn_{0.4}Fe_{0.6-x}Al_x)_2$

Table 3
The average hyperfine interaction parameters (4.2 K) for $Dy(Mn_{0.4}Fe_{0.6-x}Al_x)_2$

Composition x	n	IS (mm/s)	μ_0H_{hf} (T)	QS (mm/s)
0	5.6	0.070 (9)	17.34 (5)	0.012 (3)
0.1	5.0	0.114 (65)	14.24 (6)	0.016 (8)
0.2	4.4	0.116 (20)	10.42 (7)	0.002 (19)
0.3	3.8	0.168 (21)	8.69 (7)	0.005 (18)
0.4	3.2	0.212 (35)	7.29 (8)	−0.003 (23)
0.5	2.6	–	–	–
0.6	2.0	–	–	–

Note: n: average number of 3d electrons; IS: isomer shift; μ_0H_{hf}: magnetic hyperfine field and QS: quadrupole interaction parameter.

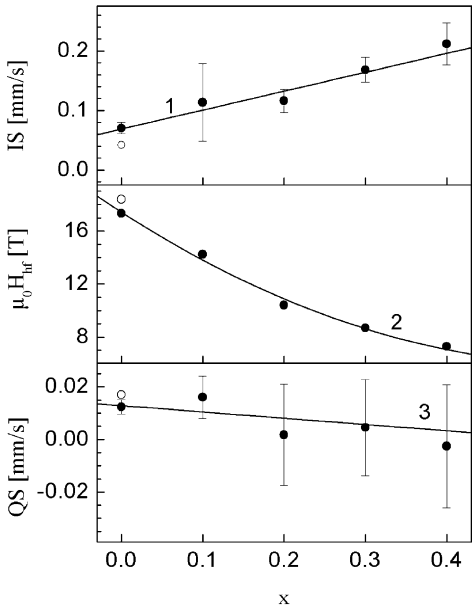

Fig. 5. Average hyperfine interaction parameters of the $Dy(Mn_{0.4}Fe_{0.6-x}Al_x)_2$ series (4.2 K): (1) the isomer shift IS in relation to Fe-metal, 300 K; (2) the magnetic hyperfine field $\mu_0 H_{hf}$ and (3) the quadrupole interaction parameter QS. Open points after [24].

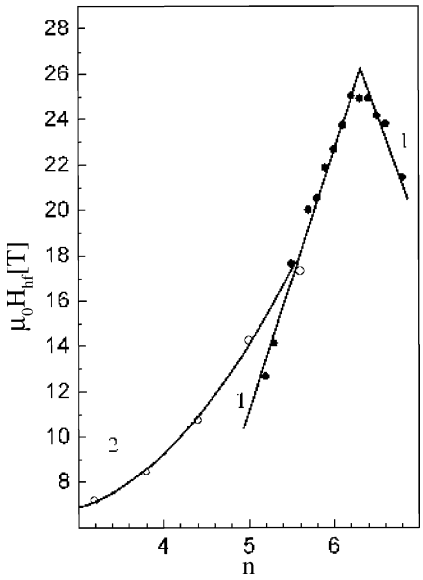

Fig. 6. Magnetic hyperfine fields $\mu_0 H_{hf}(n)$ (4.2 K) compared for series: (1) $Dy(M–M)_2$ (M–M = Mn–Fe, Fe–Co) [5,6]; (2) $Dy(Mn_{0.4}Fe_{0.6-x}Al_x)_2$.

and approaches the value 0.212(35) mm/s at $x = 0.4$. Experimental points follow the fitted formula $IS(x) = (0.317x + 0.069)$ mm/s. Considering this formula the extrapolated values of IS, 0.228 and 0.259 mm/s for $x = 0.5$ and 0.6 correspondingly, can be found. The mechanism responsible for the change in isomer shift was already discussed in detail elsewhere [10].

The magnetic hyperfine field $\mu_0 H_{hf}$ equals 17.34(5) T for $Dy(Mn_{0.4}Fe_{0.6})_2$ (this value fits well to the dependence $\mu_0 H_{hf}(y)$ observed for the $Dy(Mn_{1-y}Fe_y)_2$ series [6]) and decreases considerably with the Al-content x to the value 7.29(8) T for $x = 0.4$. The line through the experimental points corresponds to a weakly nonlinear fit: $\mu_0 H_{hf}(x) = (33.72x^2 - 39.44x + 17.43)$ T. Taking into account the above fields and corresponding to them the iron contents in the compounds, it can be found that the magnetic hyperfine field is approximately reduced by 4.18 T per one Fe atom removed from the nearest neighbourhood as a result of the Al substitution. This reduction rate is higher as compared to the change of the magnetic hyperfine field with n_2 (Fig. 4) which equals 2.42 T per Fe nearest neighbour atom.

The quadrupole interaction parameter QS adopts small values and it is expected that slightly decreases with x, if it varies at all [line is the fit: $QS(x) = (-0.024x + 0.013)$ mm/s]. Comparing Figs. 3 and 5, it can be noticed that the hyperfine parameters, IS, $\mu_0 H_{hf}$ and QS observed locally in dependence of the Fe-content in the nearest neighbourhood (the number n_2) change analogously to the average parameters observed against the Fe-content $(0.6 - x)$ in the $Dy(Mn_{0.4}Fe_{0.6-x}Al_x)_2$ series.

4. The branch of the Slater–Pauling curve

The 3d/3d Slater–Pauling curve $\mu_0 H_{hf}(n)$, a result of the substitution of one transition metal by the other, observed for the $Dy(M–M)_2$ compounds (M–M = Mn–Fe, Fe–Co), discussed previously elsewhere [5,6], is presented in Fig. 6 (line 1) for a comparison with the data of the $Dy(Mn_{0.4}Fe_{0.6-x}Al_x)_2$ series. The experimentally obtained field $\mu_0 H_{hf}(n)$ for the $Dy(Mn_{0.4}Fe_{0.6-x}Al_x)_2$ series is presented in Fig. 6 (line 2). In this case the average number of 3d electrons calculated per one site of the transition metal sublattice can be expressed as $n(x) = 0.4 \times 5 + (0.6 - x) \times 6$ where 5, 6 are numbers of 3d electrons of the Mn, Fe atom, respectively. As mentioned above, aluminium atom introduces $3s^2p^1$ electrons instead of $3d^64s^2$ electrons of transition metal Fe atom. It can be seen that as a result of the Fe/Al substitution the field $\mu_0 H_{hf}(n)$ creates a new 3d4s/3sp branch which bifurcates from the 3d/3d Slater–Pauling curve. The field of this new branch falls down nonlinearly with decreasing n. Line 2 is fitted using formula $\mu_0 H_{hf}(n) = (1.22x^2 - 6.19x + 14.44)$ T.

5. Summary and discussion

The 3d sub-bands of the starting compound $Dy(Mn_{0.4}Fe_{0.6})_2$ of the $Dy(Mn_{0.4}Fe_{0.6-x}Al_x)_2$ series are filled-up only partially and even the majority 3d sub-band is far from completeness. The value of the ^{57}Fe magnetic hyperfine field observed for the $Dy(Mn_{0.4}Fe_{0.6})_2$ compound is situated at the left branch of the 3d/3d Slater–Pauling curve (Fig. 6) and is relatively distanced from the top area of the $\mu_0 H_{hf}(n)$ fields (curve 1). In the $Dy(Mn_{0.4}Fe_{0.6-x}Al_x)_2$ series the Fe/Al substitution was used in order to enforce changes in the 3d band

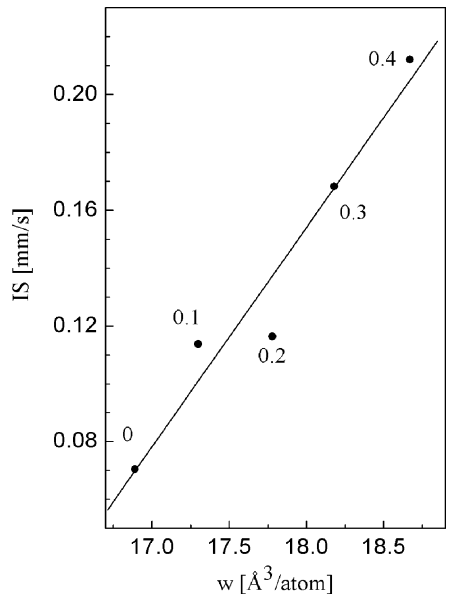

Fig. 7. The correlation between the isomer shift IS and the average volume w per atom; the experimental points are attended by the corresponding x-values.

in the case when the contribution of manganese remains constant across the series.

As a result of the Fe/Al substitution a number of changes in the 3d band is expected to appear [15,16]. At least, there is no doubt, that the Al substitution should change the Fermi energy, the width of bands and the energy shift between sub-bands [15,16].

The number of iron atoms in the transition metal sublattice is decreased, the crystal distance $d_{M–M}$ (Table 1) between the transition metal atoms as nearest neighbours increases, a mean, statistically originated, distance $D_{M–M}$ among the transition metal atoms increases, the volume w per atom increases, and consequently, as discussed elsewhere [32], the overlap of the 3d-wave functions of the neighbouring transition metal atoms is reduced. In effect, the 3d electrons are partially withdrawn from the band and the 3d-electron densities at the iron atoms area increase with x [12,13,33].

It is already known that an increase of the 3d-electron density at a given 3d atom (particularly iron atom) leads to a rise of the isomer shift observed at ^{57}Fe [33]. Fig. 7 shows a correlation between the isomer shift IS(x) and the crystal volume $w(x)$ calculated per atom which supports the above idea [10].

The dependence of the IS parameter on the 3d-electron density can be observed also locally. Namely, the Al substitution reduces in the local n.n. surroundings the number n_2 of Fe atoms for any x parameter and, as it is expected, increases locally the 3d-electron density at the studied Fe atom. Consequently an increasing tendency of the IS-parameter with decreasing n_2 is observed (Fig. 3). It seems that this increasing tendency can to some extent be artificially reduced as a result of the used simplifications, i.e. the averaging of the numbers n_1 and n_3, during fitting procedure (Table 2). The next main problem to discuss below is the $\mu_0 H_{hf}(n)$ dependence.

The series $Dy(Mn_{0.4}Fe_{0.6-x}Al_x)_2$ starts from the $Dy(Mn_{0.4}Fe_{0.6})_2$ compound for which, as mentioned above, both the 3d sub-bands are filled up only partially and are far from completeness. Moreover, the changes in the 3d band are enforced by the Fe/Al substitution, but the contribution of manganese is unchanged across the series.

The reduction of the magnetic hyperfine fields with n decreasing (Fig. 6, curve 2) can be qualitatively discussed considering the rigid band model [15,16]. Although the formally calculated number n of 3d electrons per transition metal site decreases with the Al-content, it seems, that in fact there is no considerable 3d-electron density at the Al atoms, if any. A similar problem was discussed previously elsewhere [10]. It seems reasonable to assume that the 3d electrons reside mainly at the transition metal atoms and that their 3d-electron density $\rho_{3d} = \rho^+_{3d} + \rho^-_{3d}$ per atom is presumably constant across the series, or changes only moderately.The ρ^+_{3d} and ρ^-_{3d} densities correspond to the spin-up and spin-down sub-bands, respectively.

The Al substitution reduces the average number u of the magnetic nearest neighbours surrounding the probed Fe atom and thus reduces the energy shift $\Delta E \sim \sum J_{M\text{-}M}\, m_M$ (summation over magnetic nearest neighbours) between the 3d sub-bands, where $J_{M–M}$ is an exchange integral and presumably also lowers the Fermi level E_f. As a result the 3d electrons should become gradually redistributed over the 3d sub-bands and the difference between the ρ^+_{3d} and ρ^-_{3d} densities should become reduced step by step with x. Consequently, the magnetic moment m_M of the 3d-atom and thus the magnetic hyperfine field $\mu_0 H_{hf}$ should also decrease and finally the 3d4s/3sp branch of the Slater–Pauling curve is observed (Fig. 6, curve 2). There is no a satisfactory background to predict, for example, the change in position of the sub-bands in relation to the Fermi level E_f.

Since 3d-electron densities ρ^+_{3d}, ρ^-_{3d} and ρ_{3d} are unknown yet, at present a more detailed discussion is impossible. In fact, the electronic structures of the certain rare earth-transition metal compounds were previously studied theoretically and numerically and the band structures were proposed, for instance in refs. [34–36]. Unfortunately, the systematic theoretical and numerical studies of the band structure of the 3d/3d substituted series and especially of the new 3d4s/3sp substituted series are unknown yet. Thus for a more precise discussion, a knowledge of the band structure of the Al-substituted intermetallic series is necessary. For this purpose, future sound theoretical and numerical studies would be helpful.

Acknowledgements

Supported partially by Polish Committee of Scientific Studies, grant no. 4T08D03322. M. Mróz and T. Winek are acknowledged for technical assistance.

References

[1] K.N.R. Taylor, Adv. Phys. 20 (1971) 551.
[2] K.H.J. Buschow, in: E.P. Wohlfarth (Ed.), Ferromagnetic Materials, vol. 1, North-Holland, Amsterdam, 1980.
[3] E. Burzo, H.R. Kirchmayr, in: K.A. Gschneidner Jr., L. Eyring (Eds.), Handbook on the Physics and Chemistry of Rare Earths, vol. 12, North-Holland, Amsterdam, 1989.
[4] I.A. Campbell, J. Phys. F: Metal Phys. 2 (1972) L47.
[5] B. Gicala, J. Pszczoła, Z. Kucharski, J. Suwalski, Phys. Lett. A185 (1984) 491.
[6] B. Gicala, J. Pszczoła, Z. Kucharski, J. Suwalski, Solid State Commun. 96 (1995) 511.
[7] C.E. Johnson, M.S. Ridout, T.E. Cranshaw, Phys. Rev. Lett. 6 (1961) 450.
[8] C.E. Johnson, M.S. Ridout, T.E. Cranshaw, Proc. Phys. Soc. 81 (1963) 1079.
[9] R.M. Bozorth, Ferromagnetism, Van Nostrand, Princeton, 1968.
[10] J. Pszczoła, B. Winiarska, J. Suwalski, Z. Kucharski, J. Alloys Compounds 265 (1998) 15.
[11] J. Pszczoła, B. Gicala, J. Suwalski, J. Alloys Compounds 274 (1998) 47.
[12] H. Maletta, G. Crecelius, W. Zinn, J. de Phys. (Suppl. 35) (1974) C-6-279.
[13] J. Pszczoła, J. Żukrowski, J. Suwalski, Z. Kucharski, M. Łukasiak, J. Magn. Magn. Mater. 40 (1983) 197.
[14] J. Bara, A. Pędziwiatr, W. Zarek, D. Konopka, U. Gacek, J. Magn. Magn. Mater. 27 (1982) 159.
[15] J.M. Ziman, Principles of the Theory of Solids, Cambridge University Press, London, 1972.
[16] W. Vonsovskij, Magnetizm, Nauka, Moscow, 1971 (in Russian).
[17] P. Stoch, M. Onak, J. Pszczoła, A. Pańta, J. Suwalski, Acta Phys. Polon., in press.
[18] H.M. Rietveld, J. Appl. Cryst. 2 (1969) 65.
[19] B.T.M. Willis, A. Albinati, in: International Tables for Crystallography, vol. C, Kluwer Academic Publishers, Dordrecht, 1992.
[20] J. Rodriguez-Carvajal, Physica B192 (1993) 55.
[21] F. Laves, Naturwissenschaften 27 (1939) 65.
[22] J. Chojnacki, Structural Metallography, Śląsk Press, Katowice, 1966.
[23] Z. Bojarski, E. Łągiewka, Röntgen Structural Analysis, Silesian University Press, Katowice, 1995 (in Polish).
[24] B. Gicala, J. Pszczoła, Z. Kucharski, J. Suwalski, Nukleonika 39 (1994) 195.
[25] W. Feller, An Introduction to Probability Theory and its Applications, Wiley, New York, 1961.
[26] J. Krawczyk, J. Pszczoła, Z. Kucharski, J. Suwalski, J. Alloys Compounds 219 (1995) 203.
[27] G.K. Wertheim, V. Jaccarino, J.H. Wernick, Phys. Rev. 135 (1964) A151.
[28] D. Feder, I. Nowik, J. Magn. Magn. Mater. 12 (1979) 149.
[29] M.P. Dariel, U. Atzmony, D. Lebenbaum, Phys. Status Solidi B 59 (1973) 615.
[30] S.L. Ruby, Mössbauer Effect Methodology, (Eds.), I.J. Gruverman, C.W. Seidel, vol. 8, Plenum Press, New York, 1973.
[31] G.K. Wertheim, Mössbauer Effect, Academic Press, London, 1964.
[32] K.H.J. Buschow, J. Less-Common Metals 43 (1975) 55.
[33] F. van der Woude, G.A. Sawatzky, Phys. Rep. 12 (1974) 335.
[34] R. Coehoorn, J. Magn. Magn. Mater. 99 (1991) 55.
[35] R. Coehoorn, K.H.J. Buschow, J. Magn. Magn. Mater. 118 (1993) 175.
[36] R.F. Sabirianov, S.S. Jaswal, J. Appl. Phys. 79 (1996) 5942.